#### CONSTRAINTS ON AURORAL RADIO EMISSION FROM Y DWARFS

MELODIE M. KAO, 1 GREGG HALLINAN, 1 J. SEBASTIAN PINEDA, 2 AND DAVID STEVENSON 3

## ABSTRACT

As an initial pilot study of magnetism in Y dwarfs, we have observed the three known IR variable Y dwarfs WISE J085510.83-071442.5, WISE J140518.40+553421.4, and WISEP J173835.53+273258.9 with the Karl G. Jansky Very Large Array (VLA) from 4–8 GHz to investigate the presence of quiescent radio emission as a proxy for highly circularly polarized radio emission associated with large-scale auroral currents. Measurements of magnetic fields on Y dwarfs, currently only possible by observing auroral radio emission, are essential for constraining fully convective magnetic dynamo models. We do not detect any pulsed or quiescent radio emission, down to rms noise levels of 7.2  $\mu$ Jy for WISE J085510.83-071442.5, 2.2  $\mu$ Jy for WISE J140518.40+553421.4, and 3.2  $\mu$ Jy for WISEP J173835.53+273258.9. The fractional detection rate of radio emission from T dwarfs is  $\sim$ 10% and suggests that a much larger sample of deep observations of Y dwarfs is needed to rule out radio emission in the Y dwarf population. The significance of a single detection provides strong motivation for such a search.

Keywords: brown dwarfs — planets and satellites: aurorae — planets and satellites: magnetic fields — radio continuum: stars — stars: individual (WISE J085510.83-071442.5, WISE J140518.40+553421.4, WISEP J173835.53+273258.9) — stars: magnetic fields

<sup>&</sup>lt;sup>1</sup> California Institute of Technology, Department of Astronomy, 1200 E California Blvd, MC 249-17, Pasadena, CA 91125, USA

<sup>&</sup>lt;sup>2</sup> University of Colorado Boulder, Laboratory for Atmospheric and Space Physics, 3665 Discovery Drive, Boulder CO 80303, USA

<sup>&</sup>lt;sup>3</sup> California Institute of Technology, Division of Geological & Planetary Sciences, 1200 E California Blvd, MC 150-21, Pasadena, CA 91125, USA

#### 1. INTRODUCTION

An important outstanding problem in dynamo theory is understanding how magnetic fields are generated and sustained in fully convective objects, spanning both stars and planets. Whereas prevailing dynamo models for dwarf stars with an inner radiative zone and an outer convective envelope rely on the strong differential rotation at the interface between the two layers to power  $\alpha\Omega$  dynamos (Parker 1975), fully convective dwarfs do not support such a dynamo, but exhibit tracers of activity down to T6.5 (Gizis et al. 2000; West et al. 2008; Schmidt et al. 2015; Berger et al. 2001; Berger 2002; Burgasser & Putman 2005; Berger 2006; Phan-Bao et al. 2007; Antonova et al. 2007; McLean et al. 2012; Burgasser et al. 2013; Williams et al. 2014; Burgasser et al. 2015; Kao et al. 2016; Route & Wolszczan 2016; Pineda et al. 2016). In fact, Zeeman broadening and Zeeman Doppler imaging studies confirm average surface magnetic field magnitudes of order kilogauss on dwarfs as late as M9 (Saar 1994; Johns-Krull & Valenti 1996; Donati et al. 2006; Reiners & Basri 2007; Morin et al. 2010), and pulsed radio emission associated with ~kG fields has been observed on objects as late as T6.5 (Route & Wolszczan 2012; Kao et al. 2016; Williams et al. 2016; Route & Wolszczan 2016). Instead of the  $\alpha\Omega$  dynamo, these fully convective objects must rely on alternate dynamo mechanisms to support such fields.

A number of models for possible dynamo mechanisms in this regime have been proposed (e.g. Browning 2008; Simitev & Busse 2009; Christensen et al. 2009; Morin et al. 2011; Gastine et al. 2013) but constraining data on magnetic field strengths and topologies across a wide range of mass, age, rotation rate, and temperature are sorely lacking, particularly in the brown dwarf regime. L, T, and Y dwarfs probe the lowest end of the substellar mass and temperature space—a regime that is necessary for validating and constraining any fully convective dynamo model. In particular, even a single Y dwarf magnetic field measurement would be very significant. For example, a recent breakthrough dynamo scaling relation predicts that convected energy flux sets magnetic energy in fully convective stars through planets (Christensen et al. 2009). Any ~kilogauss Y dwarf measurement unequivocally challenges this model.

Traditional techniques that rely on Zeeman broadening have successfully measured the strength, filling factor, and large-scale field topologies of objects as late as M9 (Johns-Krull & Valenti 1996; Donati et al. 2006; Reiners & Basri 2007; Morin et al. 2010). However, rotational broadening of magnetically sensitive lines and limited sensitivity prevent these techniques from accessing L and later dwarfs (Reiners & Basri 2006).

Detections of highly circularly polarized pulsed radio emission currently provide our only window into magnetic field measurements for L, T, and Y dwarfs. This emission is attributed to the electron cyclotron maser (ECM) instability (Hallinan et al. 2007), which is also responsible for producing the auroral radio emission from all of the magnetized planets in our Solar System (Zarka 2007). This magnetic activity is distinct from the standard chromospheric heating picture, where magnetic fields locally interact with hotter and less neutral atmospheres to drive transient, small-scale currents such as magnetic reconnection events and coronal loops (). Instead, brown dwarf magnetic activity appear to be more analogous to what has been observed in Jupiter, in which tracers of magnetic activity such as  $H\alpha$  and radio emission are powered by an external source, the outer magnetosphere, via auroral current systems such as magnetosphere-ionosphere coupling currents that give rise to auroral activity (Nichols et al. 2012; Bagenal et al. 2014).

ECM emission is a very powerful tool for measuring magnetic fields, and it has provided some of the first confirmations of kilogauss fields for late M and L dwarfs (Burgasser & Putman 2005; Hallinan et al. 2006, 2007, 2008; Berger et al. 2009). While emission at the second and higher harmonics can dominate when the ratio of the plasma frequency to the electron cyclotron frequency exceeds  $\sim 0.3$  (Winglee 1985), local plasma densities in the neutral atmospheres of late L, T, and Y dwarfs indicate emission dominated by the fundamental frequency for the frequencies typically observed (a few GHz). Indeed, observations of the Solar System planets show emission at almost exactly the fundamental electron cyclotron frequency  $\nu_{\rm MHz} \sim 2.8 \times B_{\rm Gauss}$  (Treumann 2006, and references therein). ECM emission frequencies in the coolest brown dwarfs therefore uniquely and accurately identify the local magnetic field strengths in the regions of the magnetosphere from where the emission originates. Near the surface of the atmosphere, where the magnetic field is the strongest and produces the highest frequency emission, electrons begin interacting with the atmosphere and can no longer freely gyrate about the field lines, causing a sharp drop-off in the emission (Zarka 1998). This high frequency ECM emission cut-off corresponds to the lower bound of the maximum large-scale magnetic field strengths in the coolest substellar objects.

Historically, radio detections of brown dwarfs are very rare; previous radio surveys encompassing objects later than M7 have yielded a  $\sim 10\%$  detection rate (Berger 2006), and until 2016, only one detection out of  $\sim 60$  L6 or later targets (Antonova et al. 2013; Route & Wol-

szczan 2013). In a previous study, we developed a selection strategy for biasing survey targets based on possible optical and infrared tracers of auroral activity (Kao et al. 2016). Our selection process was motivated by (a) low-amplitude I-band variability detected in known auroral radio emitters (Harding et al. 2013); (b) simultaneous radio and optical spectroscopic observations of an M8.5 dwarf showing Balmer line and optical broadband continuum variability tracking auroral radio pulses (Hallinan et al. 2015); and (c) predictions of increased emission at K-band or longer wavelengths from localized atmospheric heating (e.g. an impacting auroral current) (Morley et al. 2014).

Using our selection strategy, we detected highly circularly polarized radio emission for four of five pilot targets at 4–8 GHz, confirming >2.5 kG magnetic fields. By carefully comparing the magnetic field measurements derived from radio emission to measurements derived from Zeeman broadening and Zeeman Doppler imaging, we provided tentative evidence that the dynamo operating in this mass regime may be inconsistent with predicted values from Christensen et al. (2009). This suggested that parameters beyond convective flux may influence magnetic field generation in brown dwarfs.

To access the strongest constraints on fully convective dynamo models, pushing magnetic field measurements to Y dwarfs and eventually exoplanets such as hot Jupiters is critical. While previous searches for radio emission from exoplanets have been attempted, this paper is the first such attempt for Y dwarfs and is motivated by the success of our above described selection strategy and recent discoveries of variability at near- and/or mid-infrared bands for three Y dwarfs, WISE J140518.39+553421.3, WISE J085510.83-071442.5, and WISEP J173835.52+273258.9 (Cushing et al. 2016; Esplin et al. 2016; Leggett et al. 2016). These detections of variability have been quite reasonably attributed to variations in atmospheric temperature/opacity (weather), but it has been argued that similar phenomena can be driven by auroral currents for the  $\sim 10\%$  of objects that exhibit radio pulsing (Hallinan et al. 2015; Kao et al. 2016; Pineda et al. 2017). If so, aurora may play a role in some cloud variability cases but not all, as the radio fractional detection rates are low (Route 2016) compared cloud phenomena, where up to  $\sim 80\%$  of L/T transition brown dwarfs may be strong variables and  $\sim 60\%$  of L and T dwarfs outside of spectral types L9-T3.5 may be more moderate variables (Radigan et al. 2014).

In exoplanets, the primary driver of auroral emission is expected to be the interaction of the planetary magnetosphere with the stellar wind, and emission intensities therefore depend strongly on incident stellar wind flux (Gallagher & Dangelo 1981; Gurnett et al. 2002). Attempts to detect hot Jupiter radio emission have thus far been unsuccessful (e.g. Hallinan et al. 2013; Murphy et al. 2015; Bower et al. 2016).

In isolated brown dwarfs, the likely drivers for auroral emission include the co-rotation breakdown of a plasma sheet in the brown dwarf magnetosphere (Hill 2001; Cowley & Bunce 2001) or the current generated by the relative motion of a planetary satellite with respect to the brown dwarf magnetosphere (Zarka 2007). As such, radio power from isolated brown dwarfs is not limited by incident stellar wind flux but instead depends on plasma availability and the voltage drop generated across auroral current systems driven by large-scale magnetic fields (Nichols et al. 2012). If Y dwarfs have atmospheres similar to gas giant planets, predicted atmospheric ionization fractions would be sufficient for auroral current systems to form (Helling et al. 2013; Rodriguez-Barrera et al. 2015). If the generation of strong large-scale magnetic fields is indeed dependent on convected energy (i.e. temperature) as suggested by Christensen et al. (2009), early Y dwarf radio detection fractions may be unlikely to depart precipitously from the  $\sim 10\%$  detection fraction observed to be constant for L0-T6.5 (Pineda 2016; Route & Wolszczan 2016, and references therein), as brown dwarfs spend their lifetimes gravitationally contracting and cooling along the L-T-Y spectral sequence.

We present here an initial pilot study of three nearby exemplar Y dwarfs with evidence of IR variability.

# 2. TARGETS

For our study, we observed the three known IRvariable Y dwarfs. Our selection strategy is motivated by the success of our previous survey, in which we detected both pulsed and quiescent radio emission in 5/6 late L and T dwarfs by selecting for tracers of auroral emission at other wavelengths (Kao et al. 2016), specifically  $H\alpha$  and infrared variability. Although neither of the targeted Y dwarfs have confirmed  $H\alpha$  emission, their IR variability is similar in nature to that of SIMP J01365662+0933473 (hereafter SIMP0136), a clearly periodic and high-amplitude IR variable T-dwarf lacking H $\alpha$  emission (Pineda et al. 2016) that exhibited  $\sim 200 \mu \text{Jy}$  ECM pulses in our previous survey. Although clouds in brown dwarf atmospheres have been proposed to interpret observed photometric and spectroscopic variability (Marley et al. 2010; Burgasser et al. 2014; Apai et al. 2013), the Kao et al. (2016) results point to the possibility that an additional variability mechanism may be at play in some cases, e.g. extreme variables like SIMP0136, as postulated by Hallinan et al.

Table 1. Targets

Object Name	Tame Abbrev.		Parallax	Distance	$\mu_{\alpha}\cos\delta$	$\mu_{\delta}$	Ref.
	Name		(mas)	(pc)	(mas/yr)	(mas/yr)	
WISE J085510.83-071442.5	WISE 0855-07	Y	449±8	2.23±0.04	-8118±8	680±7	1-2
WISE J140518.40 $+553421.4$	WISE $1405 + 55$	Y0.5p? $^{\rm a}$	$129{\pm}19$	$7.8^{+1.3}_{-1.0}$	$-2263\pm47$	$288 \pm 41$	3-6
WISEP J173835.53+273258.9	WISE 1738+27	Y0	$128{\pm}10$	$7.8 {\pm} 0.6$	$317\pm9$	$-321 \pm 11$	4 7

<sup>&</sup>lt;sup>a</sup>Cushing et al. (2016) identified that the p? had been mistakenly dropped by Schneider et al. (2015).

References— (1) Luhman (2014); (2) Luhman & Esplin (2016); (3) Cushing et al. (2016); (4) Dupuy & Kraus (2013); (5) Cushing et al. (2011); (6) Kirkpatrick et al. (2011); (7) Beichman et al. (2014)

(2015). We stress that brown dwarf weather is much more prevalent than radio emission (Radigan et al. 2014; Route 2016; Pineda 2016), and H $\alpha$  emission and photometric variability are not correlated in L0–T8 dwarfs (Miles-Páez et al. 2017), so at least some fraction of that variability is likely causally unrelated. Target properties are listed in Table 1.

WISE J085510.83-071442.5. WISE 0855-07 was identified as a high proper motion object in the Widefield Infrared Survey Explorer (WISE) catalog (Wright et al. 2010) by Luhman (2014), with a parallax corresponding to  $\sim 2.2$  pc. The authors estimated that  $225 \text{ K} < T_{\text{eff}} < 260 \text{ K}$ , and noting that it was the reddest known T or Y dwarf, tentatively identified it as a Y dwarf. In a followup study, Faherty et al. (2014) confirmed 225 K <  $T_{\rm eff}$  < 250 K, and a tentative J3detection provided evidence that WISE 0855-07 may host sulfide and water ice clouds. The presence of atmospheric water vapor and clouds was confirmed by a  $4.5-5.2 \mu \text{m}$  spectrum obtained by Skemer et al. (2016). In contrast, Luhman & Esplin (2016) were unable to conclusively constrain the presence of clouds or nonequilibrium chemistry in its atmosphere when comparing of photometry in six optical and near-IR bands to model predictions. Finally, Esplin et al. (2016) reported variability at 3.6 and 4.5  $\mu m$  with peak-to-peak amplitudes between 3-5% and also found insufficient evidence for water ice clouds in the atmosphere. Periodicity in the observed variability was inconclusive, with periods ranging between 6.8–9.0 hr at 3.6  $\mu$ m and 5.3–9.3 hr at  $4.5 \mu m$  for two different epochs.

WISE J140518.40+553421.4. WISE 1405+55 was discovered and initially classified as a Y0p? dwarf by Cushing et al. (2011), who noted that its H-band peak was  $\sim$ 60 Å redder than the Y0 spectral standard. They estimated  $T_{\rm eff} \sim$ 350 K, log g  $\sim$ 5.00, and M  $\sim$ 30  $M_{\rm J}$ .

Hubble Space Telescope (HST) spectroscopy by Schneider et al. (2015) reclassified it as Y0.5, and confirmed that 350 K <  $T_{\rm eff}$  < 400 K, and 5.0 < log g < 5.5. Cushing et al. (2011) estimated the spectroscopic distance at 3.8 pc, while the estimated photometric distance is 8.6 pc (Kirkpatrick et al. 2011). Parallax measurements confirm a distance of  $7.8^{+1.3}_{-1.0}$  pc (Dupuy & Kraus 2013). WISE 1405+55 is the first Y dwarf from which photometric variability was detected, at 3.6 and 4.5  $\mu$ m with semi-amplitudes of 3.5% and a period of  $\sim$ 8.5 hr (Cushing et al. 2016). The authors reported that current cloud and hot-spot models cannot reproduce the observed variability.

WISEP J173835.53+273258.9. WISE 1738+27 was discovered by Cushing et al. (2011) and classified as a Y0 dwarf with an effective temperature of  $430^{+50}_{-40}$  K (Dupuy & Kraus 2013), and it serves as the Y0 spectral standard (Kirkpatrick et al. 2012). Its parallax of  $128\pm10$  corresponds to a distance of  $7.8\pm0.6$  pc (Beichman et al. 2014). Rajan et al. (2015) previously reported that it exhibited no statistically significant J-band variability, though they were only able to place an upper limit of <20.3\% on the amplitude. In contrast, Leggett et al. (2016) observed 4.5- $\mu$ m variability characteristic of a double sinusoid with  $6.0 \pm 0.1$  hr and  $3.0 \pm 0.1$  hr periods and peak-to-peak amplitude 3%, whereas near infrared monitoring at 1  $\mu$ m and Y and J bands are marginally consistent with a  $\sim 3.0$  hr period and amplitudes as high as  $\sim 5-30\%$ . The wavelength dependence and amplitude of the variability suggests atmospheric phenomena similar to what has been observed in the Solar System gas giant planets.

### 3. OBSERVATIONS

We observed the three Y dwarfs with the full VLA array in C-band (4–8 GHz), using the WIDAR correlator in 3-bit observing mode for 4 GHz bandwidth observa-

Table 2. Summary of observations

			Obs.	Time on	VLA	Synthesized Beam	I, V	Phase	Flux
Object	Band	Obs. Date	Block	Source	Configuration	Dimensions	RMS	Calibrator	Calibrator
	(GHz)	(M/D/Y)	(h)	(s)		$(arcsec \times arcsec)$	$(\mu Jy)$		
WISE 0855-07	4.0-8.0	05/22/2015	4.0	11862	BnA	$1.37 \times 0.73$	7.2, 2.4	J0902-1415	3C286
WISE 1405+55	4.0 – 8.0	05/16/2015	4.0	12360	$\operatorname{BnA}$	$1.38\times1.21$	2.2, 2.3	J1419+5423	$\rm 3C295^{\;a}$
WISE 1738+27	4.0-8.0	04/06/2016	2.0	5368	С	$4.04\times3.61$	3.2, 2.9	J1753+2848	3C286

<sup>&</sup>lt;sup>a</sup>3C295 was fully resolved and unsuitable for flux calibrations. Instead, we transferred flux calibrations using 3C286 of an archival measurement set containing observations of our phase calibrator.

tions. WISE 0855-07 and WISE 1405+55 comprised our initial pilot study with time blocks of 4 hours each on 22 May and 16 May 2015 respectively, during BnA configuration. WISE 1738+27 was included as a later target in a separate study, and we observed it for 2 hours on 06 April 2016 during C configuration. We summarize target observations in Table 2.

Searching for rotationally modulated auroral pulses can be time intensive, requiring more than one full rotation period to observe at least two pulses. Due to the longer rotational periods for our targets, we elected to search for quiescent radio emission as a proxy for pulsed emission, with the aim to follow up any quiescent detections for pulsed emission at a later date. This choice was motivated by the fact that detections of quiescent radio emission a 4-8 GHz accompany all previous auroral pulse detections (Hallinan et al. 2007, 2008; Burgasser & Putman 2005; Berger et al. 2009; Kao et al. 2016) and vice versa, as in the cases of pulsing dwarfs detected by Arecibo (which is insensitive to guiescent emission) when followed up with the VLA (Route & Wolszczan 2012; Williams et al. 2013; Route 2016; Williams et al. 2016). This suggests that physical processes governing the quiescent and pulsed radio components may be related, possibly sharing an electrodynamic engine. Indeed, Pineda et al. (2017) shows that  $H\alpha$  luminosities correlate with quiescent radio luminosities for known M7–T8 auroral pulse emitters.

Targeting quiescent emission brings additional advantages. While Jovian auroral emission cuts off at  $\sim 40$  MHz (14 Gauss), its quiescent emission is broadband up to a few GHz (Zarka 2007). Likewise, auroral brown dwarfs emit pulses at  $\gtrsim 4-10$  GHz (Kao et al. 2017) and quiescent emission up to  $\sim 100$  GHz (e.g. Williams et al. 2015). Y dwarf pulsed auroral and quiescent emission likely fall in these ranges. Previously, observations

spanning 10 years confirmed that the quiescent emission can be temporally stable (e.g. Hallinan et al. 2006; Gawroński et al. 2016), though we note two exceptions in the existing literature where late-type objects (M9.5 and L2.5) show long term variability in the quiescent emission (Antonova et al. 2007; Berger et al. 2010).

Results from a new study completed after these observations were taken show evidence that both auroral radio pulses and quiescent emission at higher frequencies (8–18 GHz) may be variable (Kao et al. 2017). In this study, L7.5–T6.5 dwarfs with previously observed 4–8 GHz pulsed and quiescent emission appeared to pulse more intermittently at higher frequencies while quiescent emission dropped off to undetectable levels in some cases. Higher frequencies correspond to stronger field strengths, which are closer to the surface of the brown dwarfs, and the authors speculated that conditions necessary to generate auroral radio emission (see §6) may be more variable near the surface of brown dwarfs.

Emerging evidence suggests that the coolest brown dwarfs can produce large-scale magnetic fields that are systematically stronger than leading predictions (Kao et al. 2017). In light of this, Y dwarf quiescent variability may also manifest at higher frequencies than probed by the present study, while quiescent emission may remain more persistent at lower frequencies such as C band. In the absence of detectable quiescent emission in this pilot study, future observations showing a systematically lower (or entirely absent) occurrence rate of Y dwarf quiescent radio emission would suggest systematically weaker magnetic fields and/or a systematic absence of auroral conditions.

#### 4. CALIBRATIONS

We calibrated our measurement sets using the standard VLA flux calibrator 3C286, and nearby phase cali-

**Table 3.** Summary of archival measurements sets for J1419+5423

			Flux	
Project #	Obs. Date	Block ID	Calibrator	Flux
	(M/D/Y)			(Jy)
15A-102	02/08/2015	30105159	3C286	$1.17593 \pm 0.000058$
14A-483	08/10/2014	29584695	3C286	$1.3839 \pm 0.0013$
14A-483	09/03/2014	29606143	3C286	$1.3968 \pm 0.0013$

brators. Typical full-bandwidth sensitivity at BnA configuration for 3.5 hours on source in C-band is  $1.8\,\mu\mathrm{Jy}$  and for C configuration on source in C band for 1.5 hours is  $2.7\,\mu\mathrm{Jy}$  with typical 3-bit observations reaching an absolute flux calibration accuracy of  $\sim 5\%$ . Flux calibration accuracy may be reduced and result in systematically offset flux densities when gain calibrations interpolated from the phase calibrator are not sufficient to correct for the variation of gain phases with time. To account for this, our observations alternated between a nearby phase calibrator and the target source with typical cycle times of 20 minutes, and we obtained gain solutions for the phase calibrators that varied slowly and smoothly over time, suggesting that this source of error is negligible.

We initially processed each measurement set with the VLA Calibration Pipeline, after which we flagged all remaining RFI and manually recalibrated as needed. As a rule, all data between 4.0–4.4 GHz was discarded due to extremely bright and persistent RFI. We obtained absolute flux by bootstrapping flux densities with the observed flux calibrators.

For WISE 0855-07, a nearby bright quasar with flux density  $\sim 0.3$  Jy limited initial sensitivity for the full measurement set to 153  $\mu$ Jy. After self calibrating, sensitivity increased to 7.2  $\mu$ Jy, for a dynamic range exceeding  $10^5$ . However, residual sidelobes remain in Stokes I. Additionally, there is sidelobe structure in Stokes V, which is a consequence of the brightness of the background source and the lack of polarization calibrations. We did not observe polarization calibrators for our targets due to the faintness of quiescently emitting radio brown dwarfs and the high circular polarization of pulsed auroral radio emission.

Similarly for WISE 1738+27, a nearby bright object with flux density  $\sim 18\,\mathrm{mJy}$  limited initial sensitivity to 5.1  $\mu\mathrm{Jy}$ . After self calibrating, sensitivity increased to 3.2  $\mu\mathrm{Jy}$ . For WISE 1405+55 we kept initial flags from

the calibration pipeline before proceeding with a manual calibration.

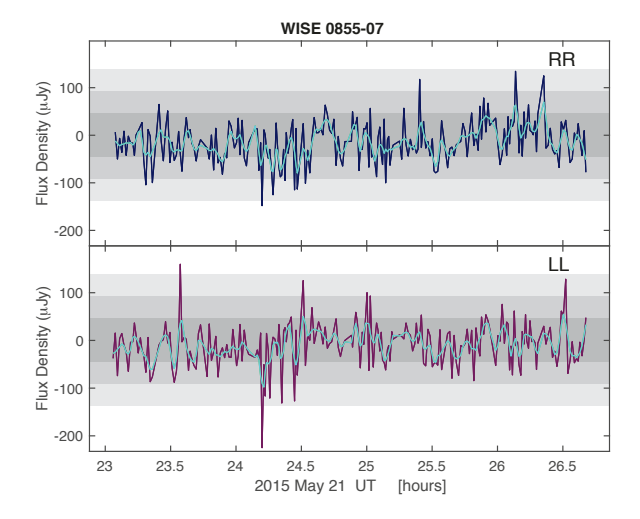
Flux calibrator 3C295 was observed for WISE 1405+55, but it was fully resolved and could not be used to satisfactorily flux calibrate. Instead, we located the measurement set nearest in time to our observations in the VLA archive containing observations of the same phase calibrator that we used, quasar J1419+5423. observations were taken on 08 February 2015 in B configuration at C band using 3C286 as a flux calibrator. After flux calibrating J1419+5423 with 3C286 in this archived measurement set, we transferred the flux calibrations to the phase calibrator field in our own measurement set, from which we then determined bandpass solutions. We also calibrated two other archival measurement sets from 10 August 2014 and 03 September 2014 containing observations of J1419+5423 at C band in D configuration to check for time variability in its flux density. Measurements of the J1419+5423 flux densities in all epochs are listed in Table 3. Based on the above ~month timescales, we expect the measured flux of J1419+5423 and therefore WISE 1405+55 to be accurate within  $\sim 20\%$ .

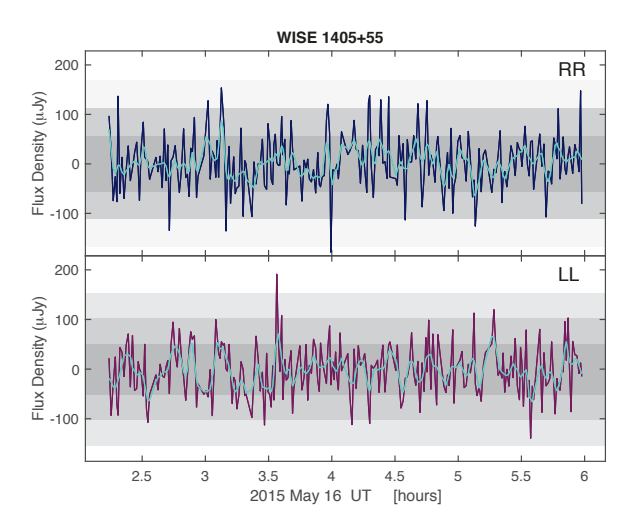
#### 5. RESULTS

Table 4. Imaging and Timeseries Results

	$3\sigma$ Upper Limit	$3\sigma$ Upper Limit	
Object	Stokes I	Stokes V	Pulse
	$(\mu \mathrm{Jy})$	$(\mu \mathrm{Jy})$	(#)
WISE 0855-07	<21.6	< 7.2	0
WISE 1405+55	< 6.6	< 6.9	0
WISE 1738+27	< 9.6	< 8.7	0

We produced Stokes I and Stokes V images of each object (total and circularly polarized intensities, respectively) with the CASA clean routine, modeling the sky emission frequency dependence with two terms and using natural weighting. We searched for a point source at the proper motion-corrected coordinates of each target. We fitted an elliptical Gaussian point source to the cleaned image of each object at its predicted coordinates using using the CASA task <code>imfit</code> but did not measure statistically significant flux densities. An examination by eye confirms the lack of a point source. Table 4 gives the  $3\sigma$  upper limits on the flux density for each source. We did not detect any radio emission from any Y dwarf





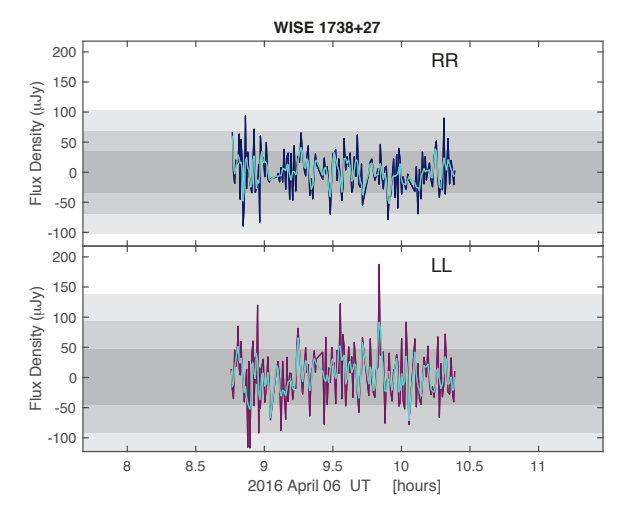


**Figure 1.** Timeseries of rr- and ll-correlated (blue and red, respectively) flux densities averaged over 30 s intervals. Grey regions indicate 1- , 2-, and  $3\sigma$  rms noise. Green lines are smoothed timeseries used for identifying pulse candidates. No pulses are detected.

in the images, down to rms noise levels of 2.2  $\mu$ Jy for WISE 1405+55, 3.2  $\mu$ Jy WISE 1738+27, and 7.2  $\mu$ Jy for for WISE 0855-07.

To check for any pulsed emission that may have been averaged down to undetectable levels over the full observing block, we used CASA plotms to export 4–8 GHz, 4–6 GHz, and 6–8 GHz timeseries of the right- and left-circularly polarized emission at the expected locations for both targets with time resolutions of 10s, 30s, and 60s. Following the procedure outlined in §4.2 of Kao et al. (2017). Figure 1 shows the 4–8 GHz timeseries for each object. We do not detect any circularly polarized radio pulses or quiescent emission for any Y dwarf.

#### 6. DISCUSSION

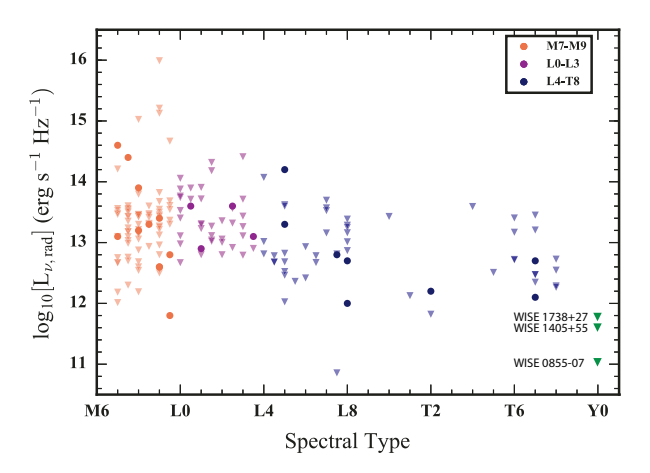


Figure 2. Quiescent emission radio luminosities as a function of spectral type. Upper limits are triangles and detections are circles. Figure adapted from Pineda et al. (2017).

Despite the decreased sensitivity in the Stokes I imaging for WISE 0855-07, the nearness of our targets allows us to place stringent constraints on their radio luminosities. We compare the  $3\sigma$  upper limits to quiescent emission flux densities observed for other radio brown dwarfs in Figure 2. These upper limits are consistent with the trend that cooler objects tend to be less radio bright than warmer ultracool dwarfs, but the data do not provide sufficient evidence for or against a break in this trend.

By itself, a lack of any detectable quiescent emission from WISE 1405+55 or WISE 1738+27 cannot unequivocally rule out any pulsed radio emission at 4–8 GHz. However, future studies demonstrating a systematic absence of detectable radio emission at these frequencies may be evidence for the onset of a dynamo distinct from those operating in late M, L, and T dwarfs. For WISE 0855-07, the rms noise that we achieved in our images is not enough to rule out the possible presence

of quiescent emission at the tens of  $\mu$ Jy level. However, we note that any quiescent radio luminosity would be an order of magnitude lower than what has previously been observed in any M7 or later brown dwarf. If the quiescent emission is not variable at these frequencies for Y dwarfs, quiescent emission in WISE 0855-07 may be unlikely. Stokes V does not suffer from the same dynamic range limitations experienced by Stokes I from the contaminating nearby bright quasar, but quiescent emission from brown dwarfs has been observed to be much less strongly circularly polarized (e.g. Burgasser & Putman 2005; Hallinan et al. 2006; Berger 2006; Hallinan et al. 2008; Berger et al. 2009; Williams & Berger 2015; Kao et al. 2016, 2017). Searching for circularly polarized pulsed emission by observing WISE 0855-07 for its full rotational period with polarization calibrations to remove spurious Stokes V sidelobe structure is the only conclusive means to rule out ECM emission from 4-8 GHz.

A detection of pulsed, circularly polarized radio emission from any of these Y dwarfs would have indicated the presence of large-scale magnetic fields of at least 2.5 kG. In the absence of any detectable radio emission from our targets, we cannot conclusively provide any strong constraints on magnetic field strengths in either object. If quiescent radio emission is indeed linked to pulsed radio emission, the following possibilities may account for why we do not observe quiescent or pulsed radio emission from our targets: (1) our targets do not produce detectable auroral radio emission and (2) currents powering auroral activity in these Y dwarfs are variable in nature. Thus far, only two late-type objects have demonstrated confirmed longterm extreme radio variability at 4-8 GHz: the L2.5 dwarf 2MASS J05233822-1403022 and the M9.5 dwarf BRI 0021 (Antonova et al. 2007; Berger et al. 2010). Three additional cool brown dwarfs exhibited undetectable quiescent emission at higher frequencies: 8-12 GHz for SDSS J04234858-0414035 (L7/T2.5 binary) down to rms noise of 1.7  $\mu$ Jy, 8–12 GHz for 2MASS J10430758+2225236 (L8) down to rms noise of 1.2  $\mu$ Jy, and >13.5 GHz for 2MASS 10475385+2124234 (T6.5) down to rms noise 3.5–5.2  $\mu \rm Jy$  for 1.5 GHz bandwidths up to 18 GHz (Kao et al. 2017). Follow-up observations are required to distinguish between quiescent emission variability or a stable drop-off.

In case (1), ECM emission will not occur if the engine for driving such emission is not present, despite the presence of sufficiently strong fields. In fact, Zeeman broadening measurements confirm mean surface field strengths in M7–M9 dwarfs that are strong enough to drive ECM emission at several GHz, yet most of these

strongly magnetized brown dwarfs have not been detected in radio (e.g. Reiners & Basri 2010; Antonova et al. 2013, and references therein). As an illustration, if the primary driver for ECM emission in isolated brown dwarfs is corotation breakdown of a plasma sheet in the magnetosphere (Cowley & Bunce 2001; Hill 2001; Bagenal et al. 2014; Badman et al. 2015, and references therein), slower rotation may prevent such corotation breakdown from occurring (Nichols et al. 2012). Indeed, Esplin et al. (2016) and Cushing et al. (2016) have reported rotational periods derived from infrared variability at 8.5 hours for WISE 0855-07, 5.3-9.3 hours for WISE 1405+55, and 3.0-6.0 hours for WISE 1738+27. In comparison, all pulsing radio brown dwarfs have reported rotational periods between 1.77 and 3.89 hours (Pineda et al. 2017, and references therein). In contrast, Jupiter and Saturn both have rotation periods between  $\sim 10-10.75$  hours (Zarka 1998), yet co-rotation breakdown powers the main auroral oval in Jupiter and dominates the Saturnian aurora (Cowley & Bunce 2001; Mauk & Bagenal 2012).

In case (2), necessary conditions for the occurrence of large-scale auroral current systems include (a) the presence of mildly relativistic populations of free electrons within the large-scale magnetospheres of our objects (b) the presence of strong, large-scale magnetic fields, and (c) the presence of a satellite magnetosphere or ionosphere for aurora generated by satellite-interactions. With regards to the first condition, sufficiently intermittent periods of volcanic activity from a satellite may cause time varying auroral activity. In the Jupiter system, vigorous volcanic activity from Io replenishes the plasma torus on a timescale of  $\sim 19$  days, and its density, temperature, and composition can vary up to a factor of two (Delamere & Bagenal 2003). Long-term monitoring show that the brightness of Jovian auroral satellite footprints (Io, Ganymede) can vary by a factor of  $\sim$ 2–10, and the brightest emission coincides with when the satellites approach the center of the plasma torus, where denser plasma is expected to generate a stronger interaction. (GéRard et al. 2006; Serio & Clarke 2008; Grodent et al. 2009; Wannawichian et al. 2010). For the second condition, a magnetic cycle in which large-scale fields evolve into small-scale fields may cause time variation in auroral activity (e.g. Kitchatinov et al. 2014; Yadav et al. 2016; Route 2016). As an illustration of the third condition, Enceladus also can (rarely) generate a detectable auroral footprint with high amplitude variability (factor of  $\sim 3$ ) over a timescale of a few hours, which is attributed to its time-variable cryo-volcanism (Pryor et al. 2011).

While the data preclude concrete conclusions about magnetic field strengths and auroral generation mechanisms in Y dwarfs, longer-term monitoring is necessary to resolve the possibilities discussed in case (2). For case (1), a broader sample of cool dwarfs spanning a range of masses and rotation rates will provide insight into whether there are any associated dependencies for either. Given that all known radio pulsing brown dwarfs are fast rotators, an initial focus on Y dwarfs with short rotation periods would be especially compelling.

#### 7. CONCLUSIONS

We have observed three Y dwarfs known to display evidence of IR variability for radio emission due to auroral magnetospheric currents. In the interest of conserving limited telescope time resources, we elected to initially search for quiescent radio emission as a proxy for pulsed emission, aiming to follow up any quiescent detections with comprehensive search for pulsed emission. We did not detect any radio emission. Targets such as WISE 0855-07 that have nearby bright contaminating radio sources will require a more methodical search for pulsed radio emission in Stokes V to rule out auroral radio emission. Follow-up observations of initially quiet targets such as WISE 1405+55 and WISE 1738+27 will be key for ruling out time variability in auroral current systems.

The limiting factor for Y dwarf radio detections is not sensitivity but rather the number of sources observed. Detection fractions for L0–L9 and T0–T6.5 spectral ranges remain constant at  $\sim 9.8\%$  (6/61) and  $\sim 10.3\%$  (4/39), and this detection fraction may extend

to early Y dwarfs as well. True fractions are likely higher, since these include surveys before the upgraded VLA and with Arecibo, which is insensitive to quiescent emission (Route & Wolszczan 2016; Pineda et al. 2017, and references therein). While quiescent radio luminosities depend weakly on spectral type (Pineda et al. 2017), selection effects bias the known Y dwarf population to be very nearby and exposure times can be adjusted to further mitigate sensitivity concerns. Assuming Y dwarf radio luminosities are ~half as faint as quiescent emission observed in late L and T dwarfs, targets  $\lesssim 10$  pc will be detectable at  $>3\sigma$  significance with 1.8  $\mu$ Jy sensitivity, which is achievable with 4 hr VLA observing blocks including overhead. Assuming early Y dwarf occurrence rates are similar to late T dwarf detection fractions, an observing program with at least ten additional targets will have a  $\sim 60\%$  chance of detecting at least one Y dwarf. Future surveys will require a combination of more objects and deeper observations to provide meaningful constraints on Y dwarfs magnetic fields.

### 8. ACKNOWLEDGEMENTS

The National Radio Astronomy Observatory (NRAO) is a facility of the National Science Foundation operated under cooperative agreement by Associated Universities, Inc.

MMK was supported by the NRAO Grote Reber Doctoral Fellowship.

JSP was supported by a grant from the National Science Foundation Graduate Research Fellowship under grant no. DGE-1144469.

Facility: JVLA

## REFERENCES

Antonova, A., Doyle, J. G., Hallinan, G., Golden, A., & Koen, C. 2007, A&A, 472, 257

Antonova, A., Hallinan, G., Doyle, J. G., et al. 2013, A&A, 549, A131

Apai, D., Radigan, J., Buenzli, E., et al. 2013, ApJ, 768, 121

Badman, S. V., Branduardi-Raymont, G., Galand, M., et al. 2015, SSRv, 187, 99

Bagenal, F., Adriani, A., Allegrini, F., et al. 2014, SSRv, 1Beichman, C., Gelino, C. R., Kirkpatrick, J. D., et al. 2014, ApJ, 783, 68

Berger, E. 2002, ApJ, 572, 503

—. 2006, ApJ, 648, 629

Berger, E., Ball, S., Becker, K. M., et al. 2001, Nature, 410, 338

Berger, E., Rutledge, R. E., Phan-Bao, N., et al. 2009, ApJ, 695, 310

Berger, E., Basri, G., Fleming, T. A., et al. 2010, ApJ, 709, 332

Bower, G. C., Loinard, L., Dzib, S., et al. 2016, ArXiv e-prints, arXiv:1608.00962

Browning, M. K. 2008, ApJ, 676, 1262

Burgasser, A. J., Melis, C., Todd, J., et al. 2015, AJ, 150, 180

Burgasser, A. J., Melis, C., Zauderer, B. A., & Berger, E. 2013, ApJL, 762, L3

Burgasser, A. J., & Putman, M. E. 2005, ApJ, 626, 486

Burgasser, A. J., Gillon, M., Faherty, J. K., et al. 2014, ApJ, 785, 48

Christensen, U. R., Holzwarth, V., & Reiners, A. 2009, Nature, 457, 167

- Cowley, S. W. H., & Bunce, E. J. 2001, Planet. Space Sci., 49, 1067
- Cushing, M. C., Kirkpatrick, J. D., Gelino, C. R., et al. 2011, ApJ, 743, 50
- Cushing, M. C., Hardegree-Ullman, K. K., Trucks, J. L., et al. 2016, ApJ, 823, 152
- Delamere, P. A., & Bagenal, F. 2003, Journal of Geophysical Research (Space Physics), 108, 1276
- Donati, J.-F., Forveille, T., Collier Cameron, A., et al. 2006, Science, 311, 633
- Dupuy, T. J., & Kraus, A. L. 2013, Science, 341, 1492
- Esplin, T., Luhman, K., Cushing, M., et al. 2016, ArXiv e-prints, arXiv:1609.05850
- Faherty, J. K., Tinney, C. G., Skemer, A., & Monson, A. J. 2014, ApJL, 793, L16
- Gallagher, D. L., & Dangelo, N. 1981, Geophys. Res. Lett., 8, 1087
- Gastine, T., Morin, J., Duarte, L., et al. 2013, A&A, 549, L5
- Gawroński, M. P., Goździewski, K., & Katarzyński, K. 2016, MNRAS, arXiv:1612.05656
- GéRard, J.-C., Saglam, A., Grodent, D., & Clarke, J. T. 2006, Journal of Geophysical Research (Space Physics), 111, A04202
- Gizis, J. E., Monet, D. G., Reid, I. N., et al. 2000, AJ, 120, 1085
- Grodent, D., Bonfond, B., Radioti, A., et al. 2009, Journal of Geophysical Research (Space Physics), 114, A07212
- Gurnett, D. A., Kurth, W. S., Hospodarsky, G. B., et al. 2002, Nature, 415, 985
- Hallinan, G., Antonova, A., Doyle, J. G., et al. 2006, ApJ, 653, 690
- —. 2008, ApJ, 684, 644
- Hallinan, G., Sirothia, S. K., Antonova, A., et al. 2013, ApJ, 762, 34
- Hallinan, G., Bourke, S., Lane, C., et al. 2007, ApJL, 663, L25
- Hallinan, G., Littlefair, S. P., Cotter, G., et al. 2015, Nature, 523, 568
- Harding, L. K., Hallinan, G., Boyle, R. P., et al. 2013, ApJ, 779, 101
- Helling, C., Jardine, M., Stark, C., & Diver, D. 2013, ApJ, 767, 136
- Hill, T. W. 2001, J. Geophys. Res., 106, 8101
- Johns-Krull, C. M., & Valenti, J. A. 1996, ApJL, 459, L95
- Kao, M. M., Hallinan, G., Pineda, J. S., Burgasser, A., & Stevenson, D. 2017, ApJ
- Kao, M. M., Hallinan, G., Pineda, J. S., et al. 2016, ApJ, 818, 24

- Kirkpatrick, J. D., Cushing, M. C., Gelino, C. R., et al. 2011, ApJS, 197, 19
- Kirkpatrick, J. D., Gelino, C. R., Cushing, M. C., et al. 2012, ApJ, 753, 156
- Kitchatinov, L. L., Moss, D., & Sokoloff, D. 2014, MNRAS, 442, L1
- Leggett, S. K., Cushing, M. C., Hardegree-Ullman, K. K., et al. 2016, ArXiv e-prints, arXiv:1607.07888
- Luhman, K. L. 2014, ApJL, 786, L18
- Luhman, K. L., & Esplin, T. L. 2016, AJ, 152, 78
- Marley, M. S., Saumon, D., & Goldblatt, C. 2010, ApJL, 723, L117
- Mauk, B., & Bagenal, F. 2012, Washington DC American Geophysical Union Geophysical Monograph Series, 197, doi:10.1029/2011GM001192
- McLean, M., Berger, E., & Reiners, A. 2012, ApJ, 746, 23
  Miles-Páez, P. A., Metchev, S. A., Heinze, A., & Apai, D. 2017, ApJ, 840, 83
- Morin, J., Donati, J.-F., Petit, P., et al. 2010, MNRAS, 2269
- Morin, J., Dormy, E., Schrinner, M., & Donati, J.-F. 2011, MNRAS, 418, L133
- Morley, C. V., Marley, M. S., Fortney, J. J., & Lupu, R. 2014, ApJL, 789, L14
- Murphy, T., Bell, M. E., Kaplan, D. L., et al. 2015, MNRAS, 446, 2560
- Nichols, J. D., Burleigh, M. R., Casewell, S. L., et al. 2012, ApJ, 760, 59
- Parker, E. N. 1975, ApJ, 198, 205
- Phan-Bao, N., Osten, R. A., Lim, J., Martin, E. L., & Ho, P. T. P. 2007, ApJ, 658, 553
- Pineda, J. S. 2016, PhD thesis, California Institute of Technology, doi:10.7907/Z90C4SRW
- Pineda, J. S., Hallinan, G., & Kao, M. M. 2017, ArXiv e-prints, arXiv:1708.02942
- Pineda, J. S., Hallinan, G., Kirkpatrick, J. D., et al. 2016, ApJ, 826, 73
- Pryor, W. R., Rymer, A. M., Mitchell, D. G., et al. 2011, Nature, 472, 331
- Radigan, J., Lafrenière, D., Jayawardhana, R., & Artigau, E. 2014, ApJ, 793, 75
- Rajan, A., Patience, J., Wilson, P. A., et al. 2015, MNRAS, 448, 3775
- Reiners, A., & Basri, G. 2006, ApJ, 644, 497
- —. 2007, ApJ, 656, 1121
- —. 2010, ApJ, 710, 924
- Rodriguez-Barrera, M. I., Helling, C., Stark, C. R., & Rice, A. M. 2015, MNRAS, 454, 3977
- Route, M. 2016, ArXiv e-prints, arXiv:1609.07761
- Route, M., & Wolszczan, A. 2012, ApJL, 747, L22

-.. 2013, ApJ, 773, 18

19001

- —. 2016, ApJL, 821, L21
- Saar, S. H. 1994, in IAU Symposium, Vol. 154, Infrared Solar Physics, ed. D. M. Rabin, J. T. Jefferies, & C. Lindsey, 437
- Schmidt, S. J., Hawley, S. L., West, A. A., et al. 2015, AJ, 149, 158
- Schneider, A. C., Cushing, M. C., Kirkpatrick, J. D., et al. 2015, ApJ, 804, 92
- Serio, A. W., & Clarke, J. T. 2008, Icarus, 197, 368 Simitev, R. D., & Busse, F. H. 2009, Europhys. Lett., 85,
- Skemer, A. J., Morley, C. V., Allers, K. N., et al. 2016, ApJL, 826, L17
- Treumann, R. A. 2006, A&A Rv, 13, 229
- Wannawichian, S., Clarke, J. T., & Nichols, J. D. 2010, Journal of Geophysical Research (Space Physics), 115, A02206
- West, A. A., Hawley, S. L., Bochanski, J. J., et al. 2008, AJ, 135, 785

- Williams, P. K. G., & Berger, E. 2015, ArXiv e-prints, arXiv:1502.06610
- Williams, P. K. G., Berger, E., & Zauderer, B. A. 2013, ApJL, 767, L30
- Williams, P. K. G., Casewell, S. L., Stark, C. R., et al. 2015, ApJ, 815, 64
- Williams, P. K. G., Cook, B. A., & Berger, E. 2014, ApJ, 785, 9
- Williams, P. K. G., Gizis, J. E., & Berger, E. 2016, ArXiv e-prints, arXiv:1608.04390
- Winglee, R. M. 1985, J. Geophys. Res., 90, 9663
- Wright, E. L., Eisenhardt, P. R. M., Mainzer, A. K., et al. 2010, AJ, 140, 1868
- Yadav, R. K., Christensen, U. R., Wolk, S. J., & Poppenhaeger, K. 2016, ApJL, 833, L28
- Zarka, P. 1998, J. Geophys. Res., 103, 20159
- —. 2007, Planet. Space Sci., 55, 598